

## SUPPLEMENTAL MATERIAL

Selective utilization of benzimidazolyl-norcobamides as cofactors by the tetrachloroethene reductive dehalogenase of *Sulfurospirillum multivorans*

Sebastian Keller<sup>1</sup>, Cindy Kunze<sup>1</sup>, Martin Bommer<sup>2</sup>, Christian Paetz<sup>3</sup>, Riya C. Menezes<sup>4</sup>, Aleš Svatoš<sup>4</sup>, Holger Dobbek<sup>2</sup>, and Torsten Schubert<sup>1</sup>

<sup>1</sup>Department of Applied and Ecological Microbiology, Institute of Microbiology, Friedrich Schiller University, Philosophenweg 12, D-07743 Jena, Germany

<sup>2</sup>Structural Biology / Biochemistry, Department of Biology, Humboldt-Universität zu Berlin, Philippstrasse 13, D-10115 Berlin, Germany

<sup>3</sup>Research Group Biosynthesis / NMR and <sup>4</sup>Research Group Mass Spectrometry, Max Planck Institute for Chemical Ecology, Hans-Knöll-Straße 8, D-07745 Jena, Germany

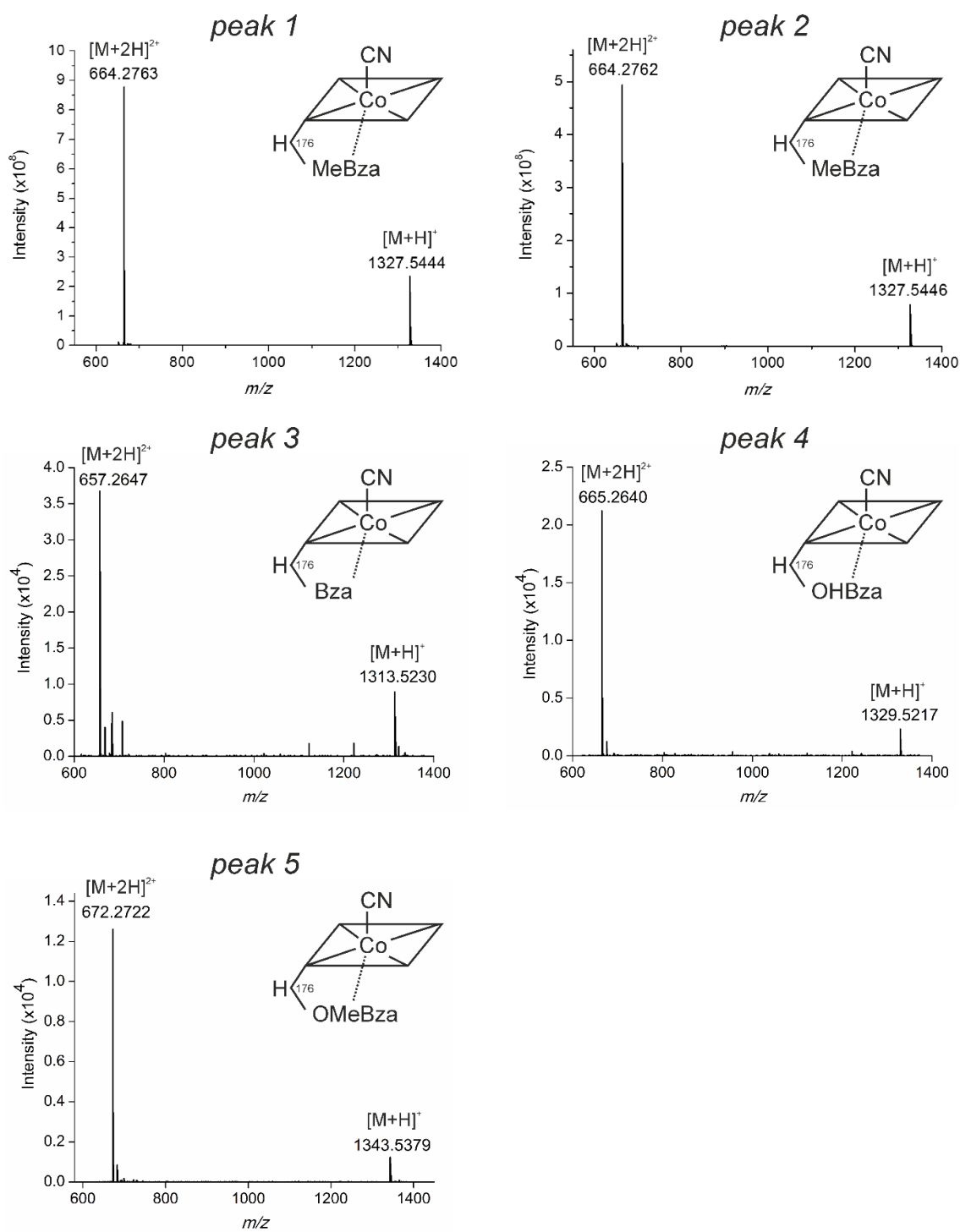


**Fig. S1:** Data from UHPLC-ESI-HRMS analysis of purified NCbas. Singly and doubly protonated ions were detected, which were assigned to the respective NCbas. Numbering of the peaks is referring to figure 1C.

**Tab. S1:** Calculated monoisotopic masses of the NCbas in comparison to the measured values. Labeling of the peaks is in accordance to figure 1C.

	Compound	Accurate mass ( <i>m/z</i> )	Calculated mass ( <i>m/z</i> )	$\delta$ (ppm)	Elemental composition
Peak 1	MeBza-NCba	[M+H] <sup>+</sup> 1327.5444	1327.5434	0.752	C <sub>61</sub> H <sub>85</sub> O <sub>14</sub> N <sub>14</sub> CoP
		[M+2H] <sup>2+</sup> 664.2763	664.2753	1.477	C <sub>61</sub> H <sub>86</sub> O <sub>14</sub> N <sub>14</sub> CoP
Peak 2	MeBza-NCba	[M+H] <sup>+</sup> 1327.5446	1327.5434	0.888	C <sub>61</sub> H <sub>85</sub> O <sub>14</sub> N <sub>14</sub> CoP
		[M+2H] <sup>2+</sup> 664.2762	664.2753	1.266	C <sub>61</sub> H <sub>86</sub> O <sub>14</sub> N <sub>14</sub> CoP
Peak 3	Bza-NCba	[M+H] <sup>+</sup> 1313.5230	1313.5277	-3.602	C <sub>60</sub> H <sub>83</sub> O <sub>14</sub> N <sub>14</sub> CoP
		[M+2H] <sup>2+</sup> 657.2647	657.2675	-4.205	C <sub>60</sub> H <sub>84</sub> O <sub>14</sub> N <sub>14</sub> CoP
Peak 4	OHBza-NCba	[M+H] <sup>+</sup> 1329.5218	1329.5227	-0.606	C <sub>60</sub> H <sub>83</sub> O <sub>15</sub> N <sub>14</sub> CoP
		[M+2H] <sup>2+</sup> 665.2640	665.2650	-1.460	C <sub>60</sub> H <sub>84</sub> O <sub>15</sub> N <sub>14</sub> CoP
Peak 5	OMeBza-NCba	[M+H] <sup>+</sup> 1343.5379	1343.5383	-0.429	C <sub>61</sub> H <sub>85</sub> O <sub>15</sub> N <sub>14</sub> CoP
		[M+2H] <sup>2+</sup> 672.2722	672.2728	-0.857	C <sub>61</sub> H <sub>86</sub> O <sub>15</sub> N <sub>14</sub> CoP
#	norpseudo-B <sub>12</sub>	[M+H] <sup>+</sup> 1330.5283	1330.5291	-0.607	C <sub>58</sub> H <sub>82</sub> O <sub>14</sub> N <sub>17</sub> CoP

## NMR data (extended)

**Structure analysis of the 6-OHBza-*N*- $\alpha$ -ribofuranosyl moiety of 6-OHBza-norcobamide.** All norcobamide (NCba) structures were analyzed by NMR spectroscopy with focus on the various benzimidazoles incorporated during the cultivation experiments. In the following, the structure analysis of the 6-OHBza-*N*- $\alpha$ -ribofuranosyl moiety of 6-OHBza-NCba is described as a typical example (Fig. S2-9). In an analogous manner the structures and chemical shifts of the 5-OMeBza-NCba (Fig. S10-15), the 5-MeBza-NCba (Fig. S16-21), and the 6-MeBza-NCba (Fig. S22-27) have been worked out.

The  $^1\text{H}$  NMR spectrum showed six signals in the low field range, three of them attributable to an aromatic AMX spin system. However, a deviation of the chemical shifts compared to the literature (Crofts *et al.*, 2014) was observed and thus the structure was elucidated *de novo*. Starting point was a  $^1\text{H}$ - $^{13}\text{C}$  HSQC cross signal at  $\delta_{\text{H}}$  6.17,  $m/\delta_{\text{C}}$  86.6 (Fig. S7), which was assigned to position 1' of the  $\alpha$ -ribofuranose moiety. By means of  $^1\text{H}$ - $^1\text{H}$  DQFCOSY, selective  $^1\text{H}$ - $^1\text{H}$  TOCSY (offset on H-1') and  $^1\text{H}$ - $^{13}\text{C}$  HSQC all remaining positions of the  $\alpha$ -ribofuranose were assigned (Fig. S5). The  $^1\text{H}$ - $^{13}\text{C}$  HMBC (Fig. S8) correlation of H-1' with C-2 ( $\delta_{\text{C}}$  141.8) was proving the connection of the  $\alpha$ -ribofuranosyl with the benzimidazolyl part. In order to elucidate the position of the hydroxyl group at the benzimidazole, a  $^1\text{H}$ - $^1\text{H}$  ROESY experiment was conducted (Fig. S9). Correlation of H-1' with the broad singlet of H-7 ( $\delta_{\text{H}}$  6.80) was observed, and  $^1\text{H}$ - $^{13}\text{C}$  HSQC revealed the corresponding C-7 at  $\delta_{\text{C}}$  96.8. Furthermore, H-4' ( $\delta_{\text{H}}$  4.02, *m*) showed a ROE-correlation to H-2 ( $\delta_{\text{H}}$  7.03), indicating that the  $\alpha$ -ribofuranosyl and benzimidazolyl systems have a perpendicular orientation towards each other. Because no  $^1\text{H}$ - $^1\text{H}$  DQFCOSY correlation of H-7 was observed, the

position of the hydroxyl group in the benzimidazolyl moiety had to be in position 6. The remaining protonated positions of the benzimidazole were assigned from  $^1\text{H}$ - $^{13}\text{C}$  HMBC and  $^1\text{H}$ - $^1\text{H}$  DQFCOSY correlations, respectively.  $^1\text{H}$ - $^{13}\text{C}$  HMBC correlations from H-7 revealed the chemical shifts of position 5 ( $\delta_{\text{H}}$  6.73, *d*,  $^3J_{\text{HH}}=8.9$  Hz /  $\delta_{\text{C}}$  113.2) and position 9 ( $\delta_{\text{C}}$  132.2). H-4 ( $\delta_{\text{H}}$  6.49, *d*,  $^3J_{\text{HH}}=8.9$  Hz) was determined from a  $^1\text{H}$ - $^1\text{H}$  DQFCOSY correlation with H-5. The corresponding  $^{13}\text{C}$  chemical shift C-4 ( $\delta_{\text{C}}$  117.4) was determined by  $^1\text{H}$ - $^{13}\text{C}$  HSQC. The  $^{13}\text{C}$  chemical shifts of position 8 ( $\delta_{\text{C}}$  132.5) and 6 ( $\delta_{\text{C}}$  153.7) were determined from the  $^1\text{H}$ - $^{13}\text{C}$  HMBC correlation with H-4. Finally, the  $^1\text{H}$ - $^{13}\text{C}$  HMBC correlation of H-2 with C-8 and C-9, the evidence for the linkage of the imidazolyl moiety with the phenyl moiety of benzimidazole, completed the structure elucidation of the 6-OHBza-NCba.

#### **References:**

Crofts TS, Hazra AB, Tran JL, Sokolovskaya OM, Osadchiy V, Ad O, Pelton J, Bauer S, Taga ME. 2014. Regiospecific formation of cobamide isomers is directed by CobT. *Biochemistry*. 53:7805-7815.

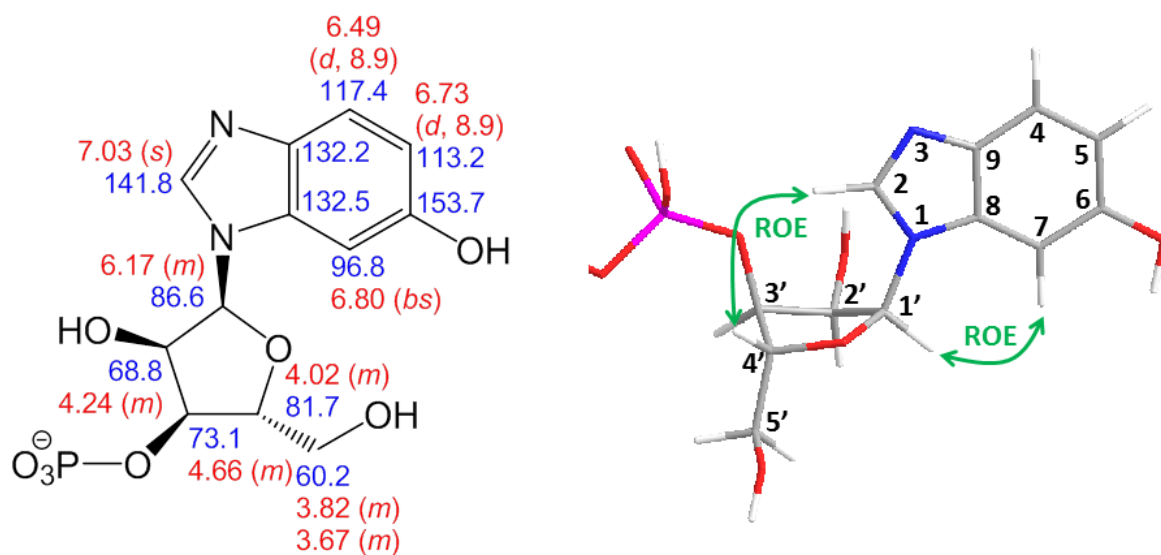


**Fig. S2:** Chemical shifts ( $\delta_H$  red,  $\delta_C$  blue) of the 6-OHBza-*N*- $\alpha$ -ribofuranosyl-fragment and the  $^1H$ - $^1H$  ROESY key correlations for determination of the position of the hydroxyl group.

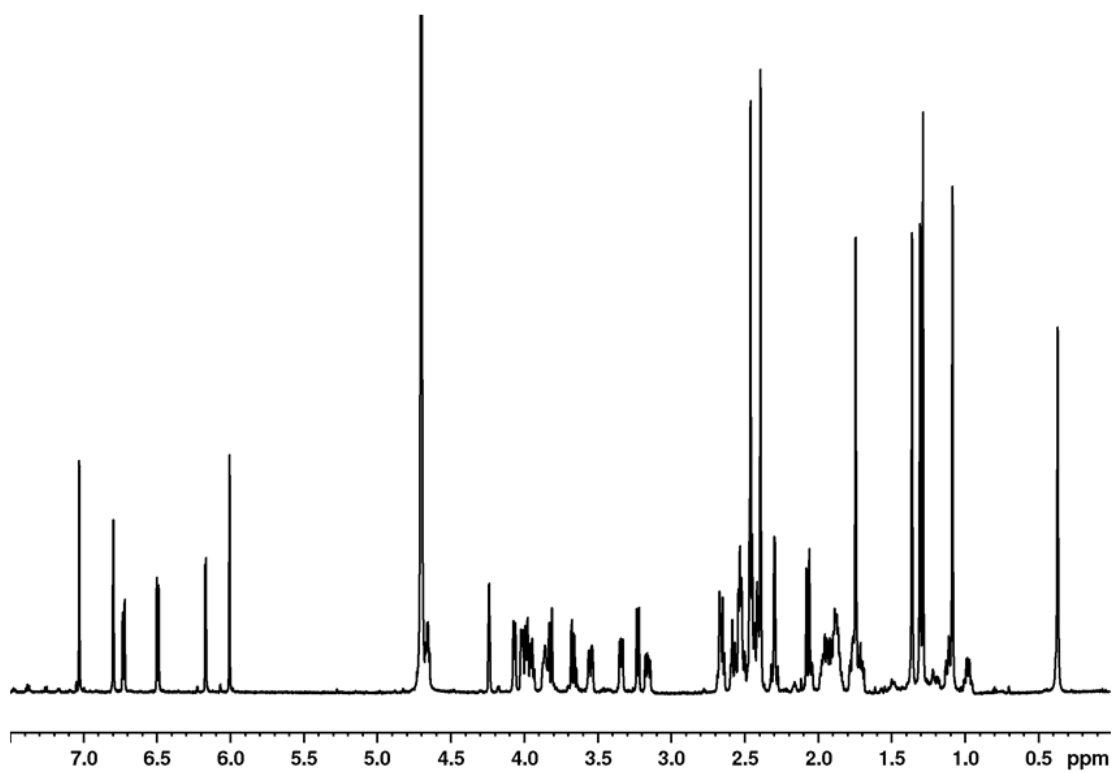


**Fig. S3:** <sup>1</sup>H-NMR spectrum of the 6-OHBza-NCba.

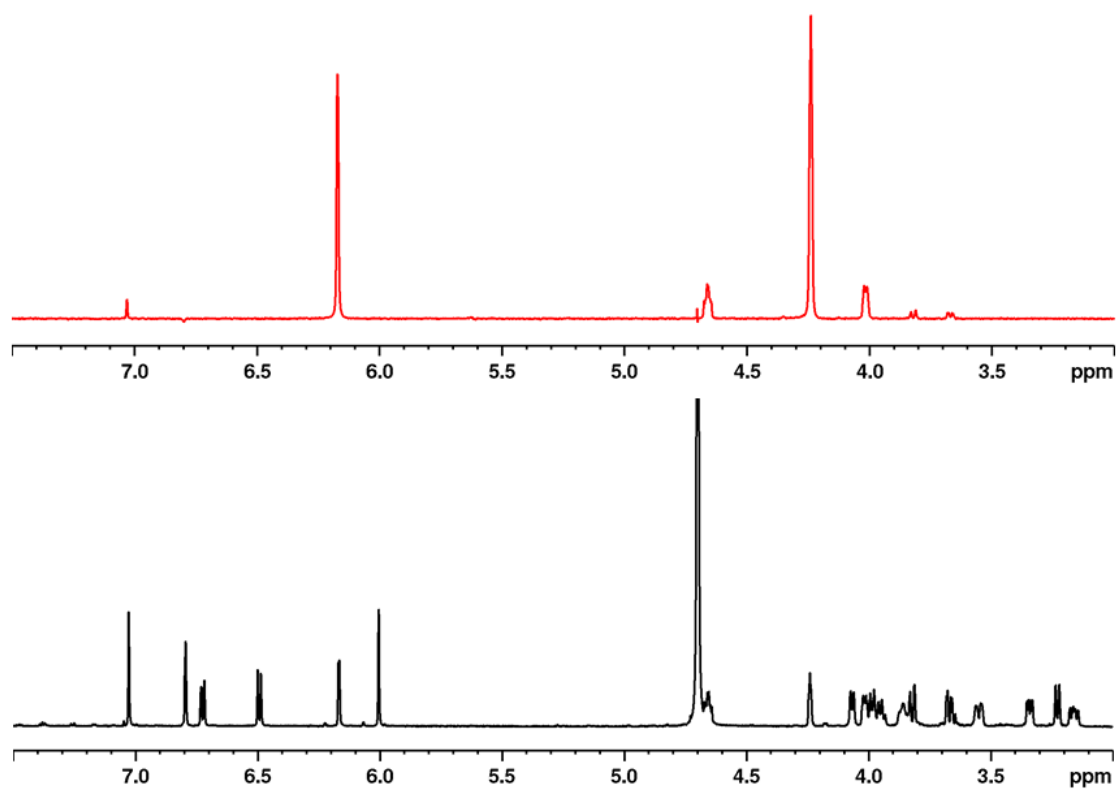


**Fig. S4:**  $^1\text{H}$ -SELTOCSY spectrum of the  $\alpha$ -ribofuranosyl moiety (red) of the 6-OHBza-NCba compared to the  $^1\text{H}$ -NMR spectrum (black) of the 6-OHBza-NCba.



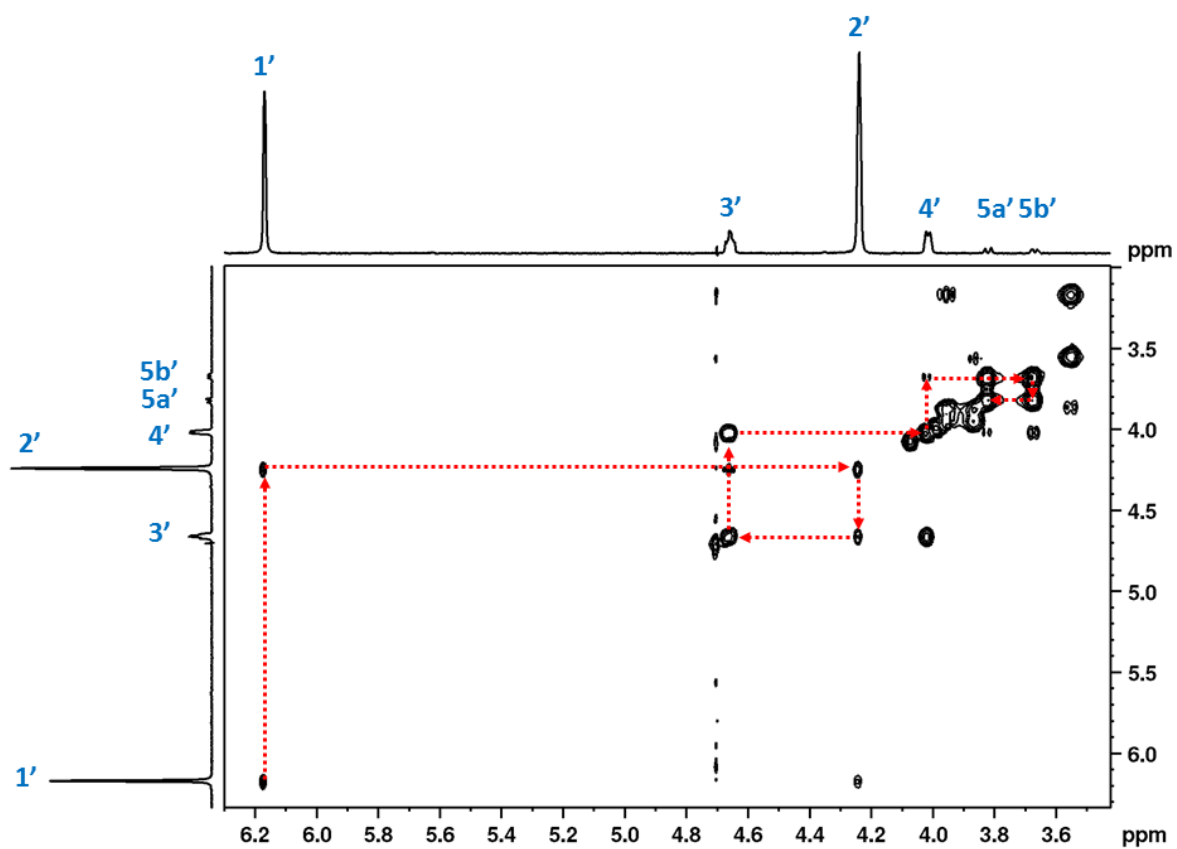


**Fig. S5:**  $^1\text{H}$ - $^1\text{H}$  DQFCOSY spectral detail of the  $\alpha$ -ribofuranosyl unit of 6-OHBza-NCba with SELTOCSY spectra as projections.

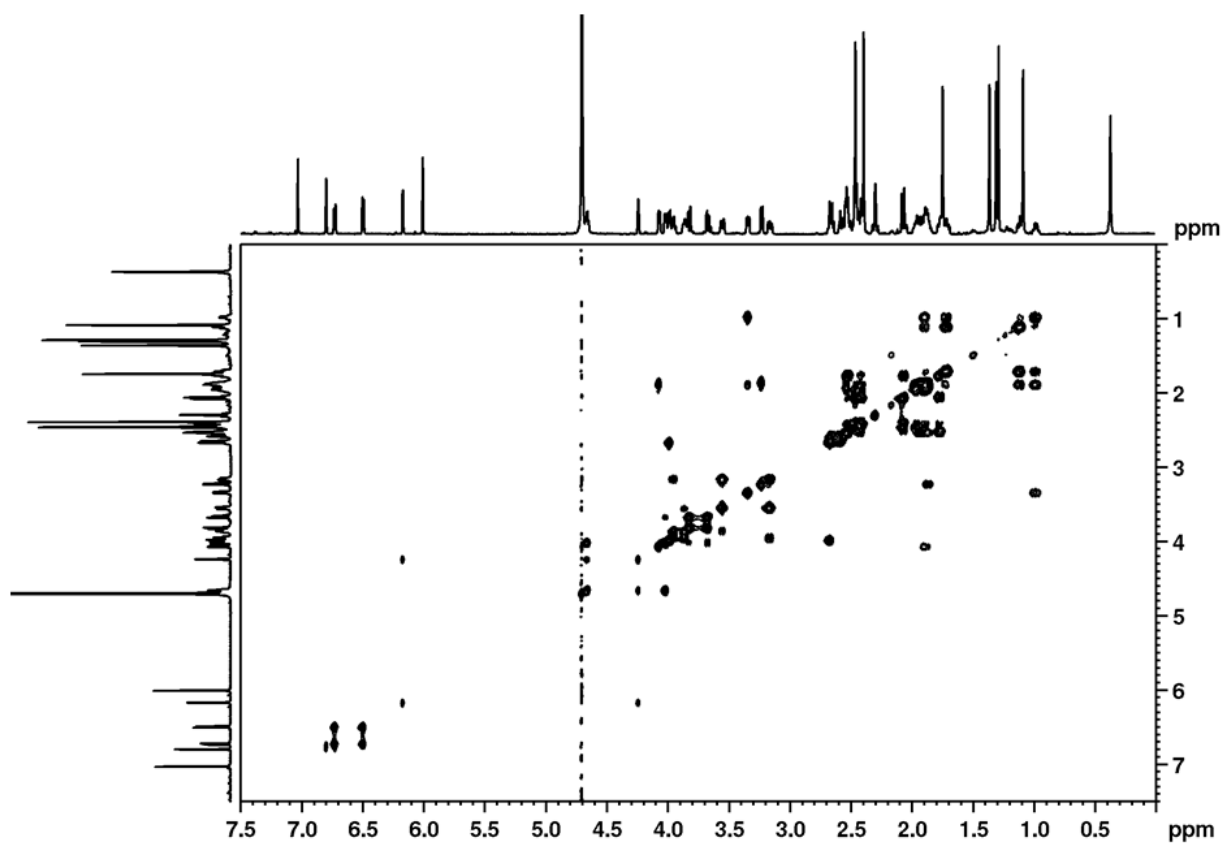


**Fig. S6:** Full  $^1\text{H}$ - $^1\text{H}$ -DQFCOSY spectrum of the 6-OHBza-NCba.

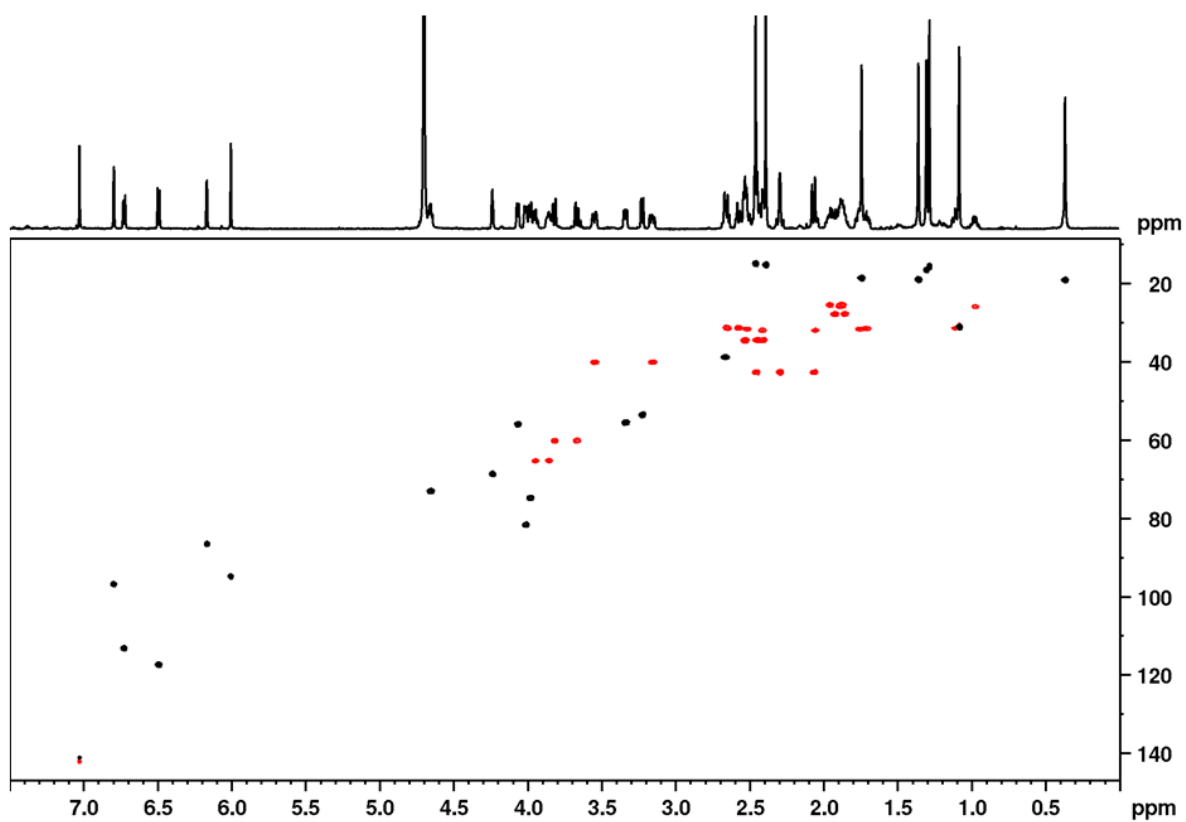


**Fig. S7:**  $^1\text{H}$ - $^{13}\text{C}$  HSQC spectrum of 6-OHBza-NCba.

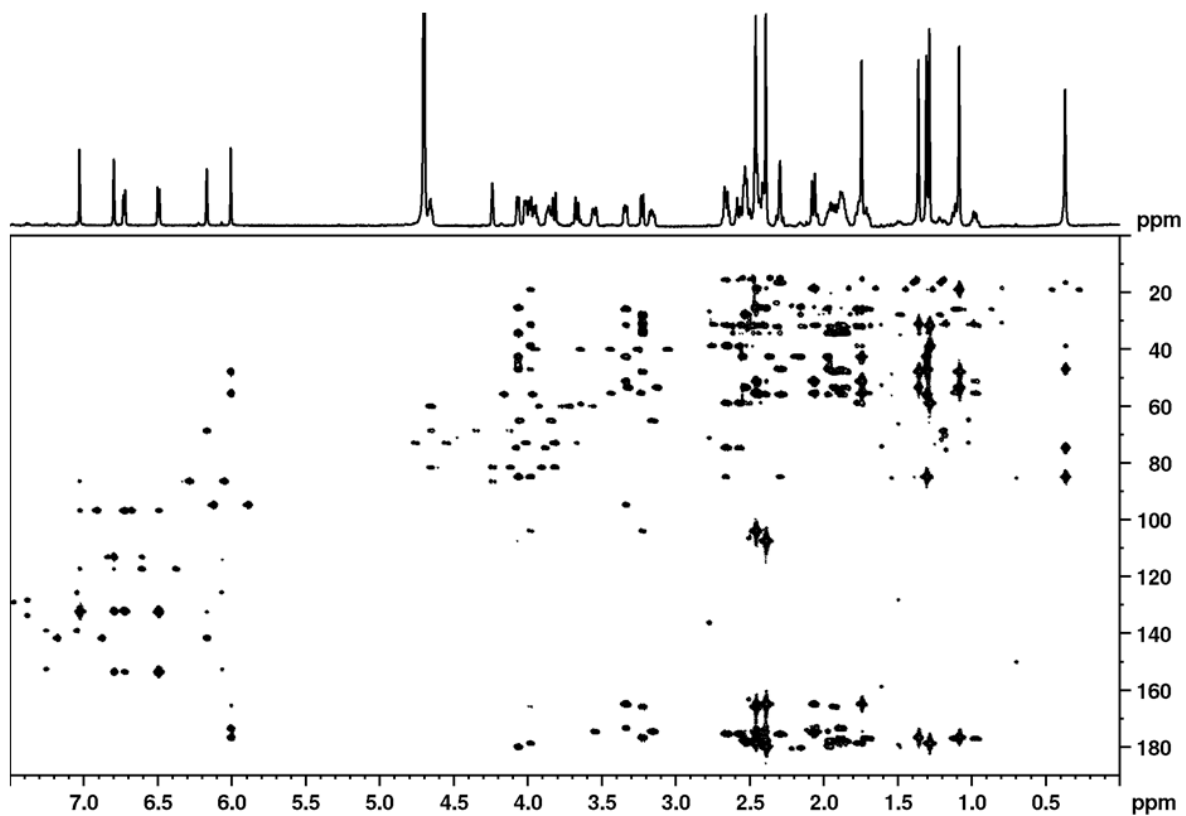


**Fig. S8:**  $^1\text{H}$ - $^{13}\text{C}$  HMBC spectrum of the 6-OHBza-NCba.

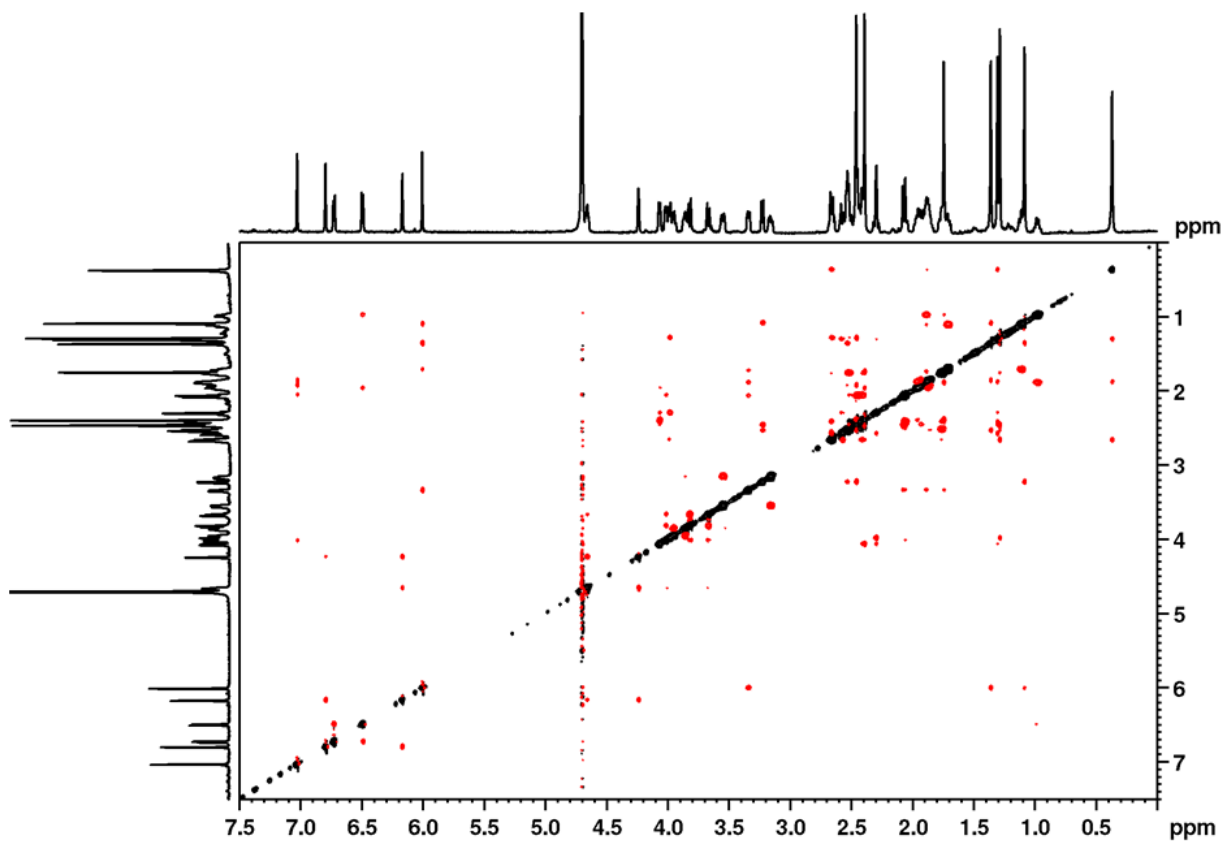


**Fig. S9:**  $^1\text{H}$ - $^1\text{H}$  ROESY spectrum of the 6-OHBza-NCba.

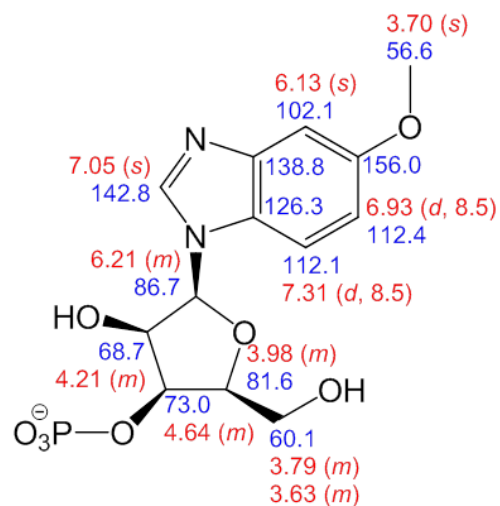


**Fig. S10:** Chemical shifts ( $\delta_{\text{H}}$  red,  $\delta_{\text{C}}$  blue) of the 5-OMeBza-*N*- $\alpha$ -ribofuranosyl- fragment.

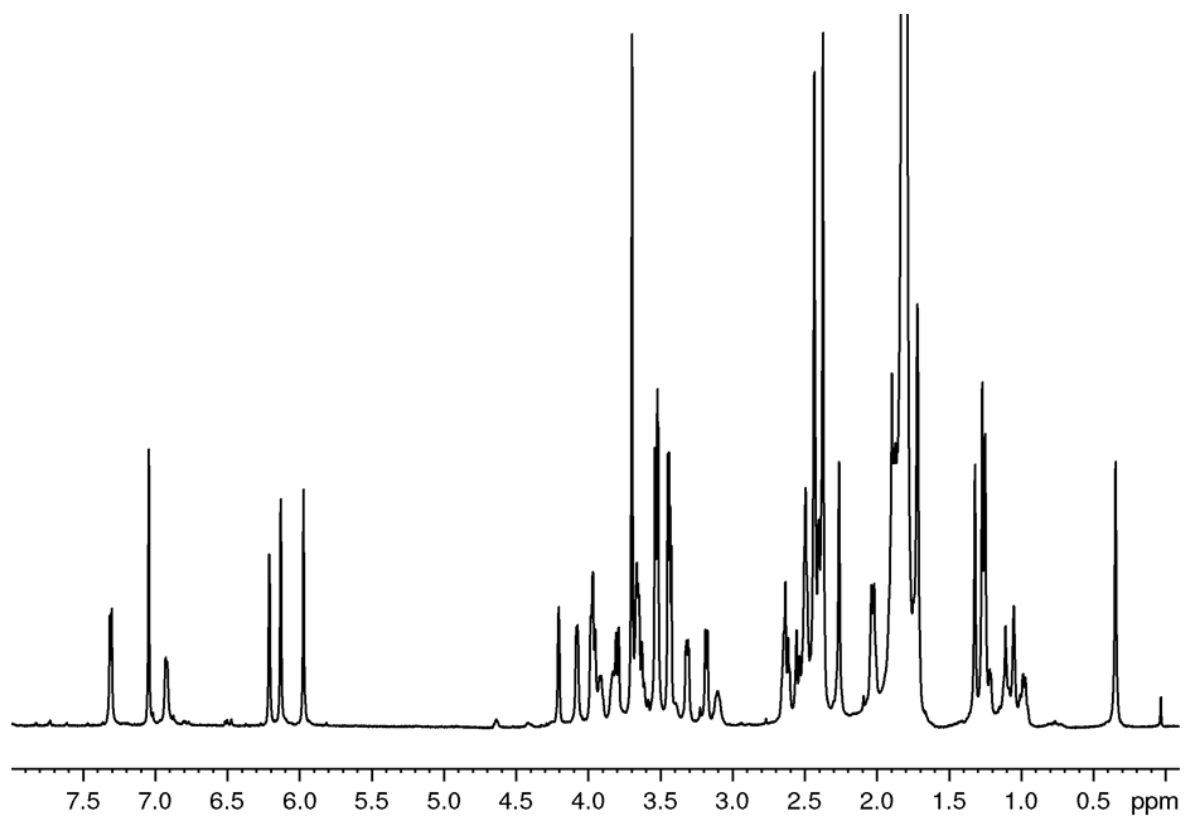


**Fig. S11:** <sup>1</sup>H-NMR spectrum of the 5-OMeBza-NCba.

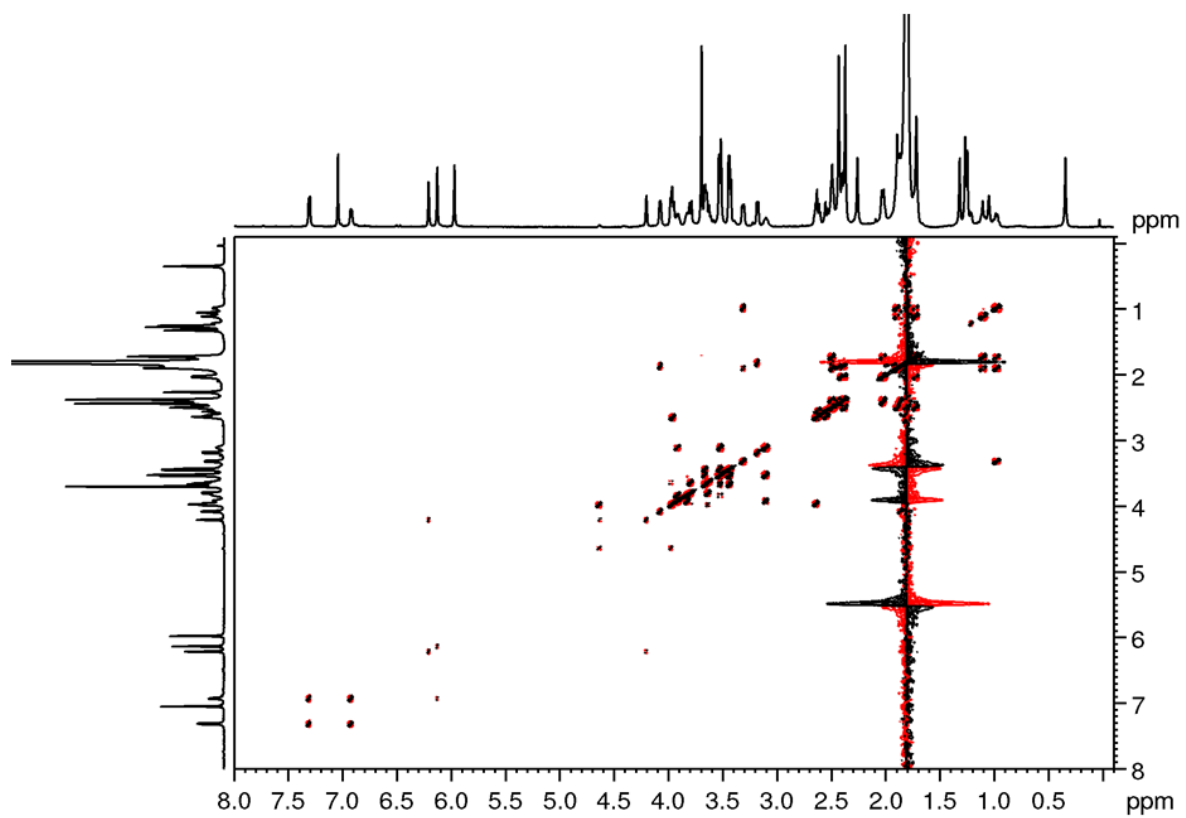


**Fig. S12:**  $^1\text{H}$ - $^1\text{H}$ -DQFCOSY spectrum of the 5-OMeBza-NCba.



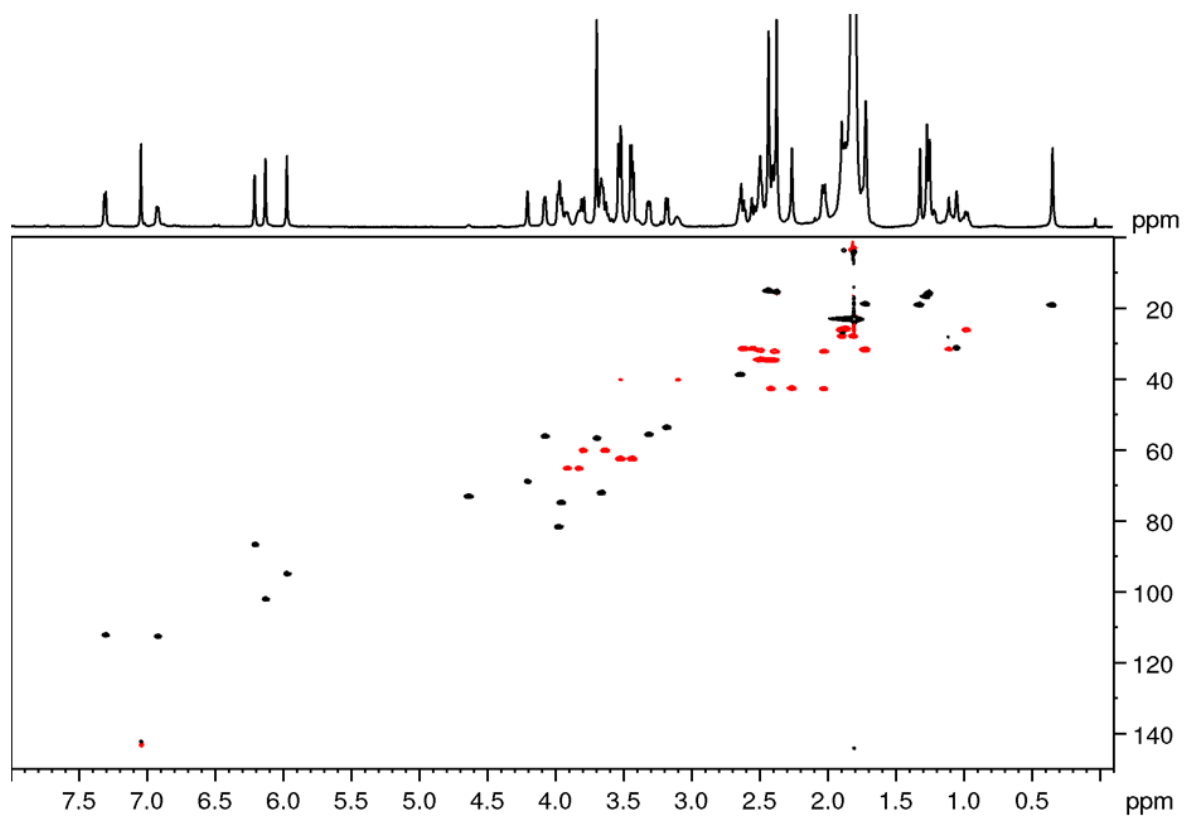


**Fig. S13:**  $^1\text{H}$ - $^{13}\text{C}$  HSQC spectrum of 5-OMeBza-NCba.

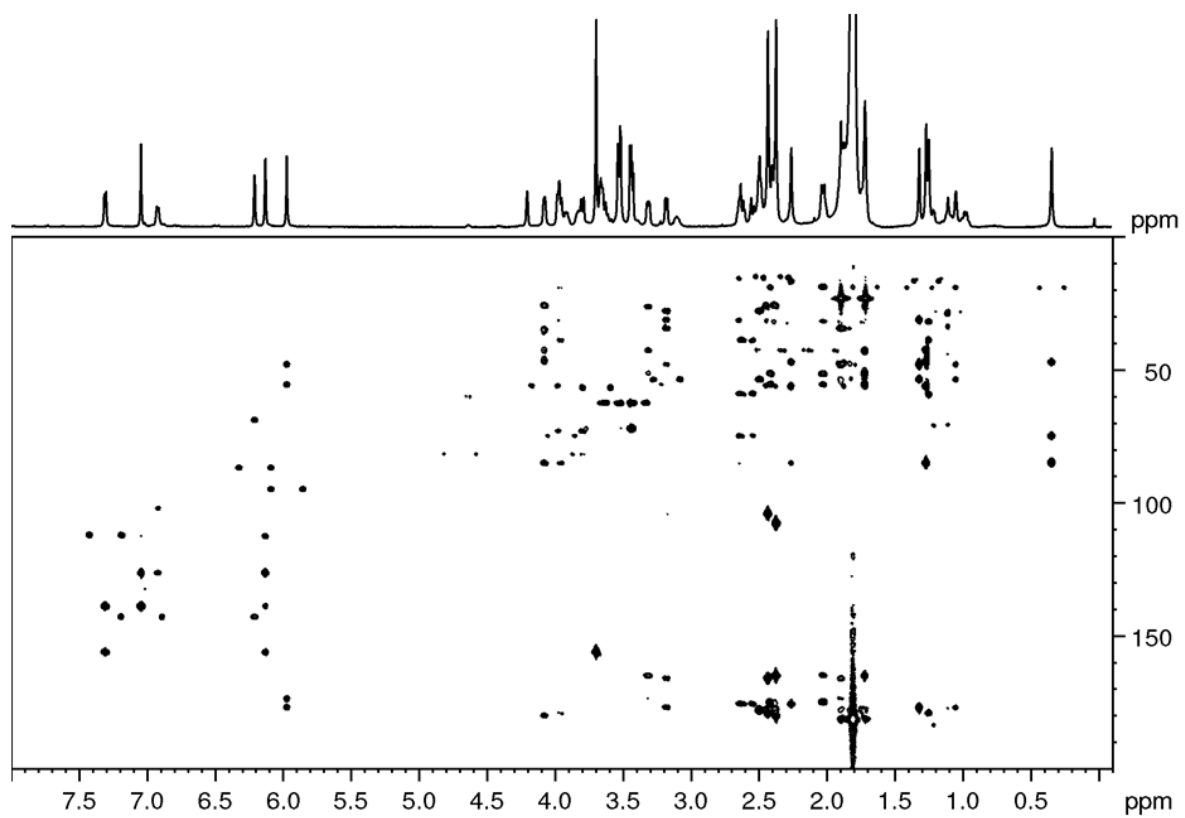


**Fig. S14:**  $^1\text{H}$ - $^{13}\text{C}$  HMBC spectrum of the 5-OMeBza-NCba.

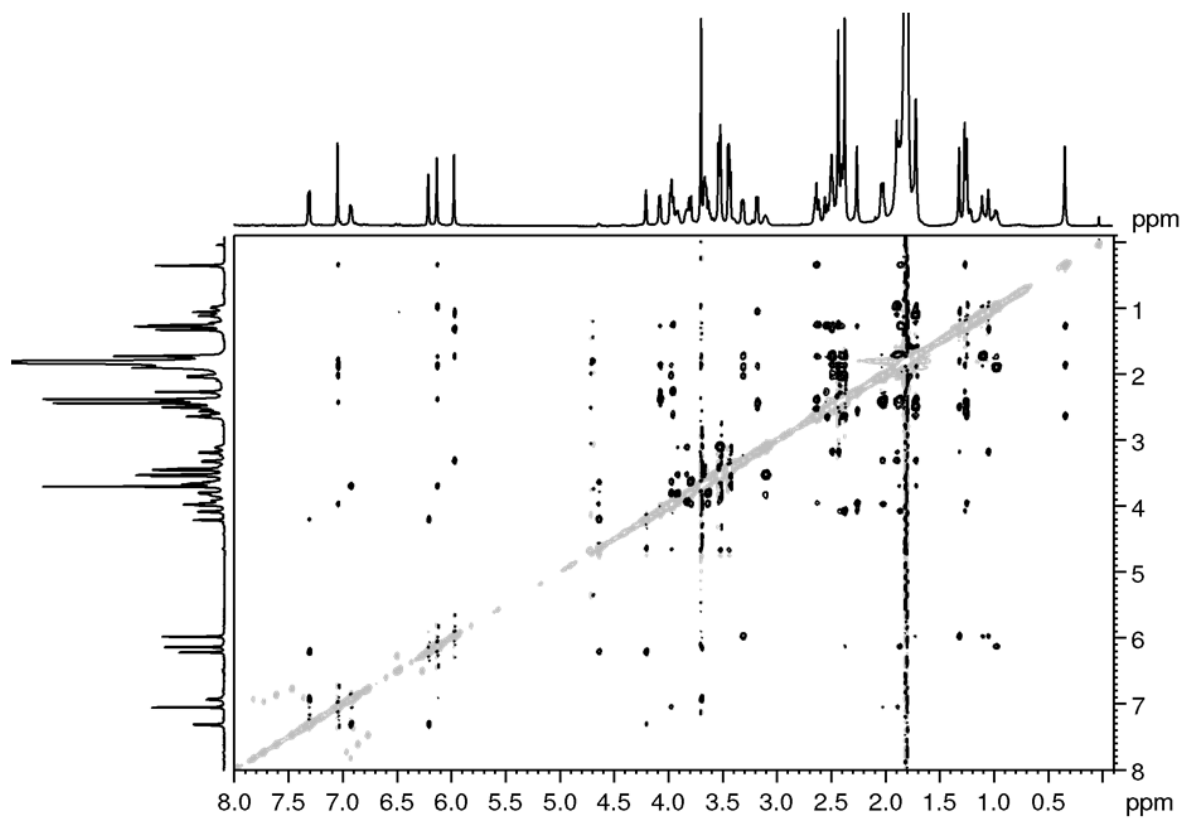


**Fig. S15:**  $^1\text{H}$ - $^1\text{H}$  ROESY spectrum of the 5-OMeBza-NCba.

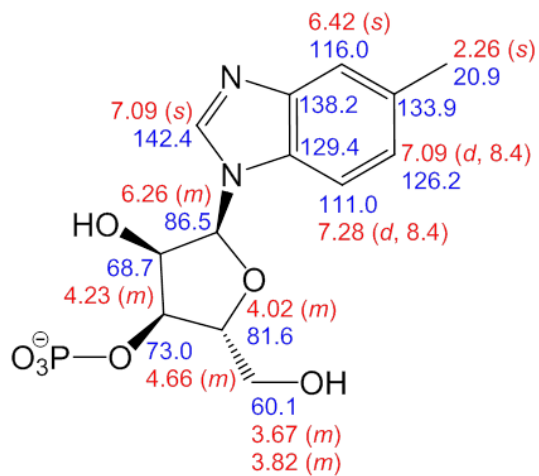


**Fig. S16:** Chemical shifts ( $\delta_{\text{H}}$  red,  $\delta_{\text{C}}$  blue) of the 5-MeBza-*N*- $\alpha$ -ribofuranosyl-fragment.

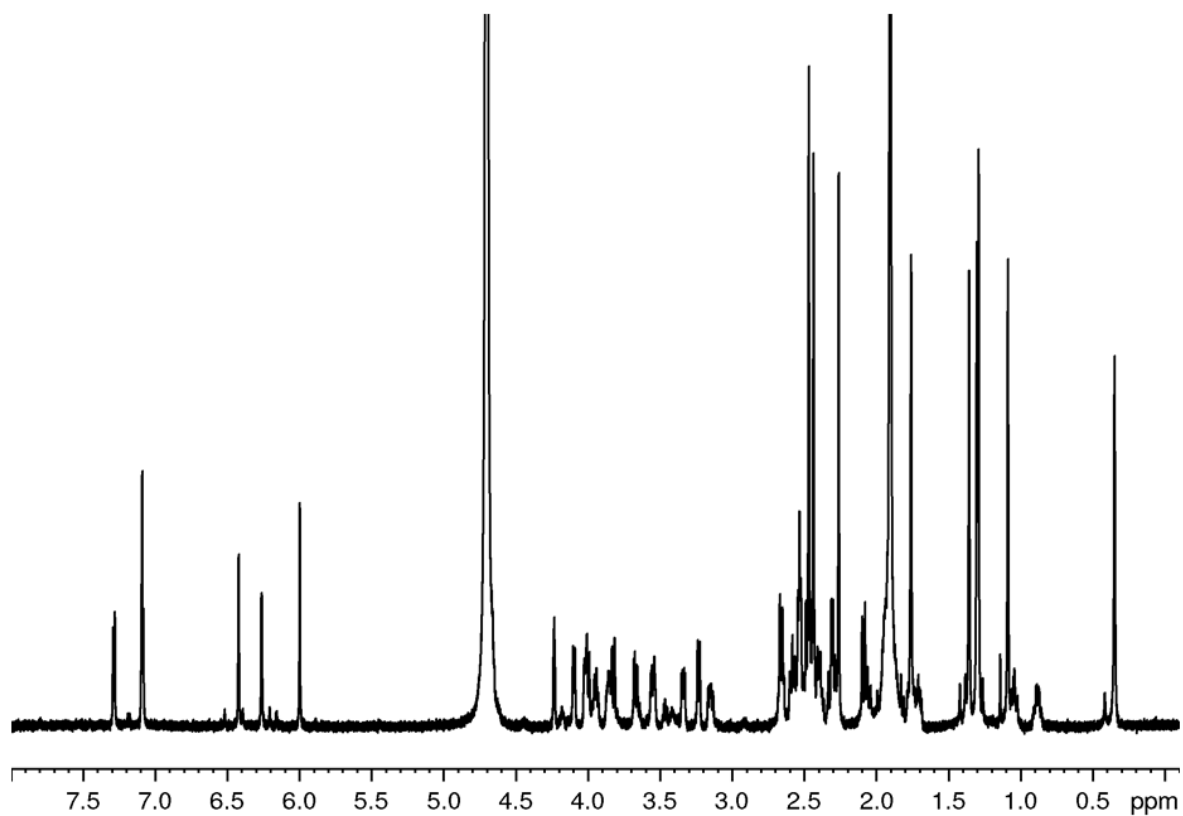


**Fig. S17:** <sup>1</sup>H-NMR spectrum of the 5-MeBza-NCba.

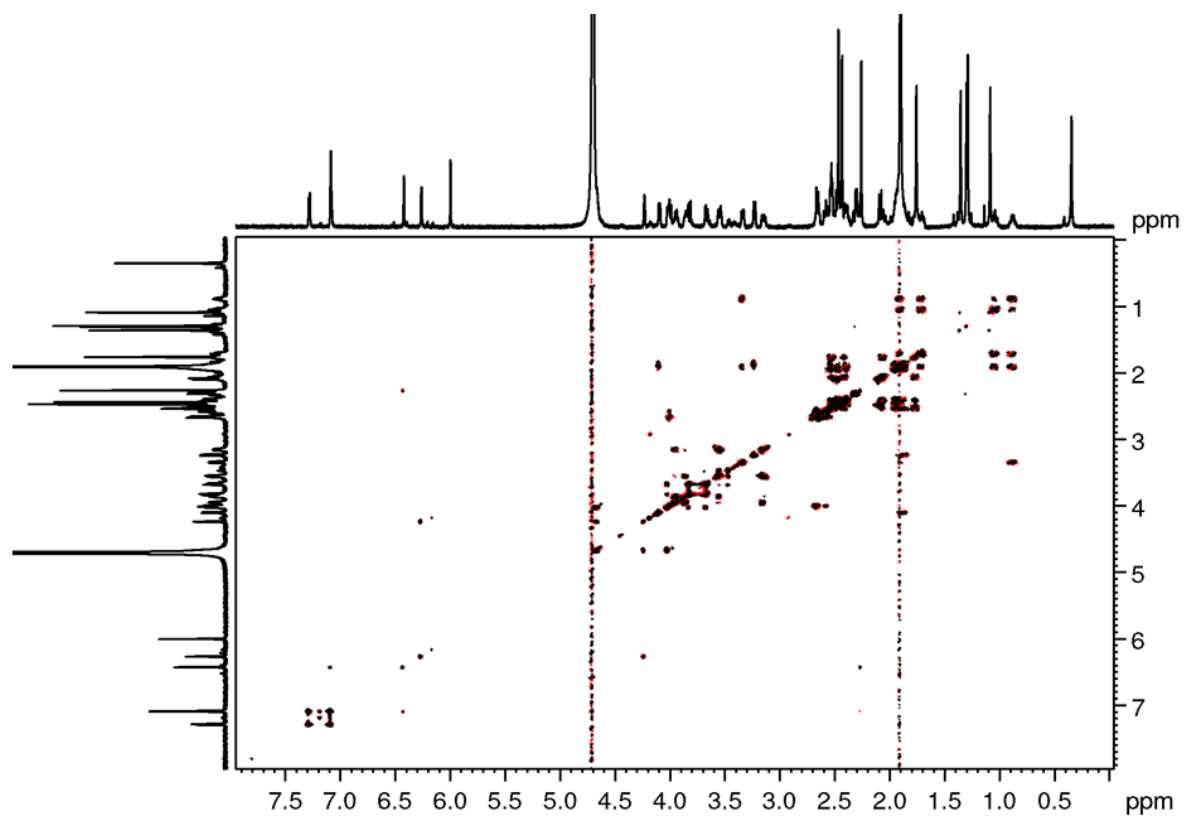


**Fig. S18:**  $^1\text{H}$ - $^1\text{H}$ -DQFCOSY spectrum of the 5-MeBza-NCba.

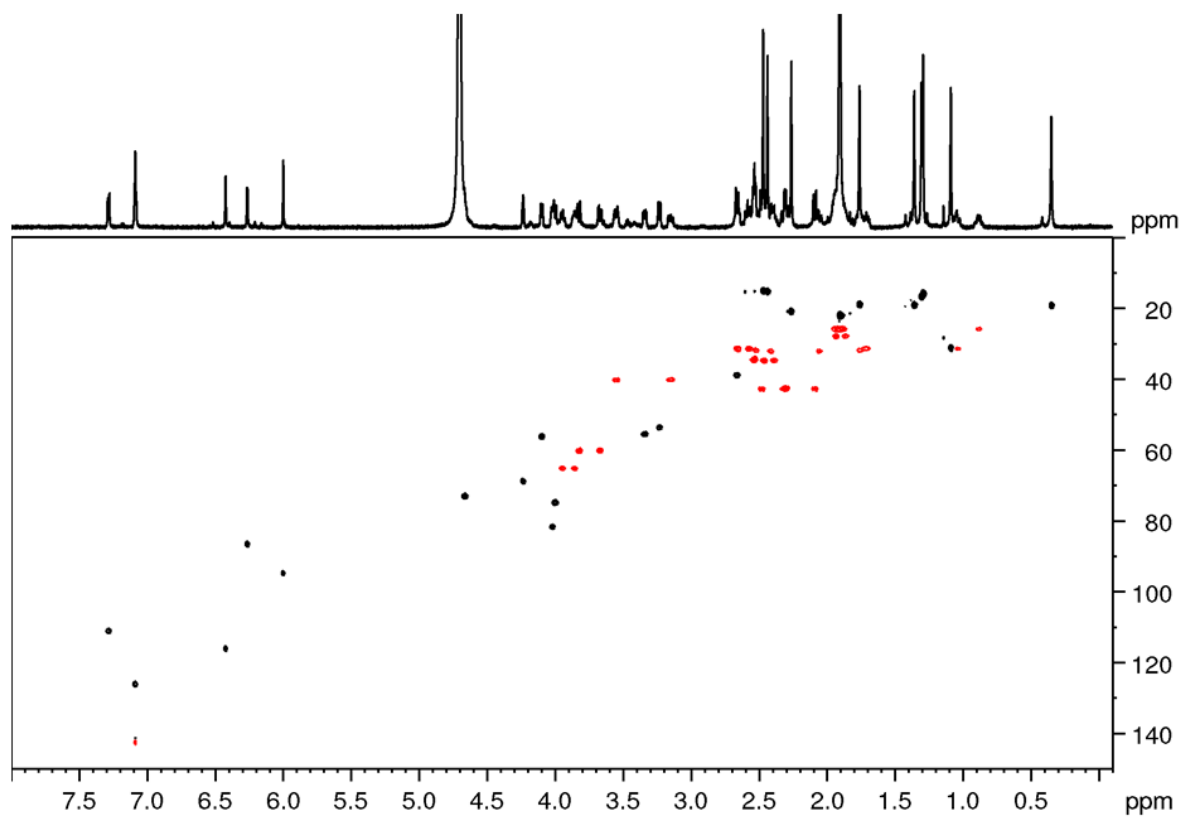


**Fig. S19:**  $^1\text{H}$ - $^{13}\text{C}$  HSQC spectrum of 5-MeBza-NCba.

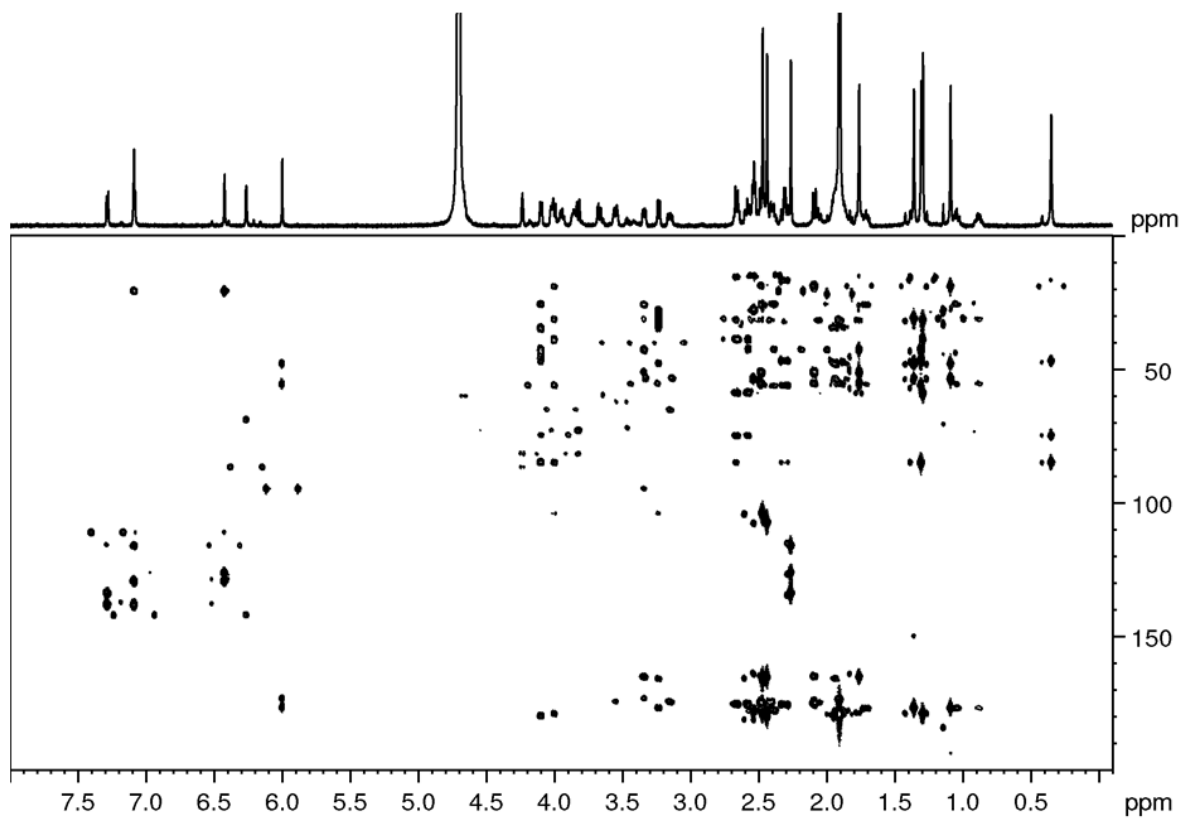


**Fig. S20:**  $^1\text{H}$ - $^{13}\text{C}$  HMBC spectrum of the 5-MeBza-NCba.



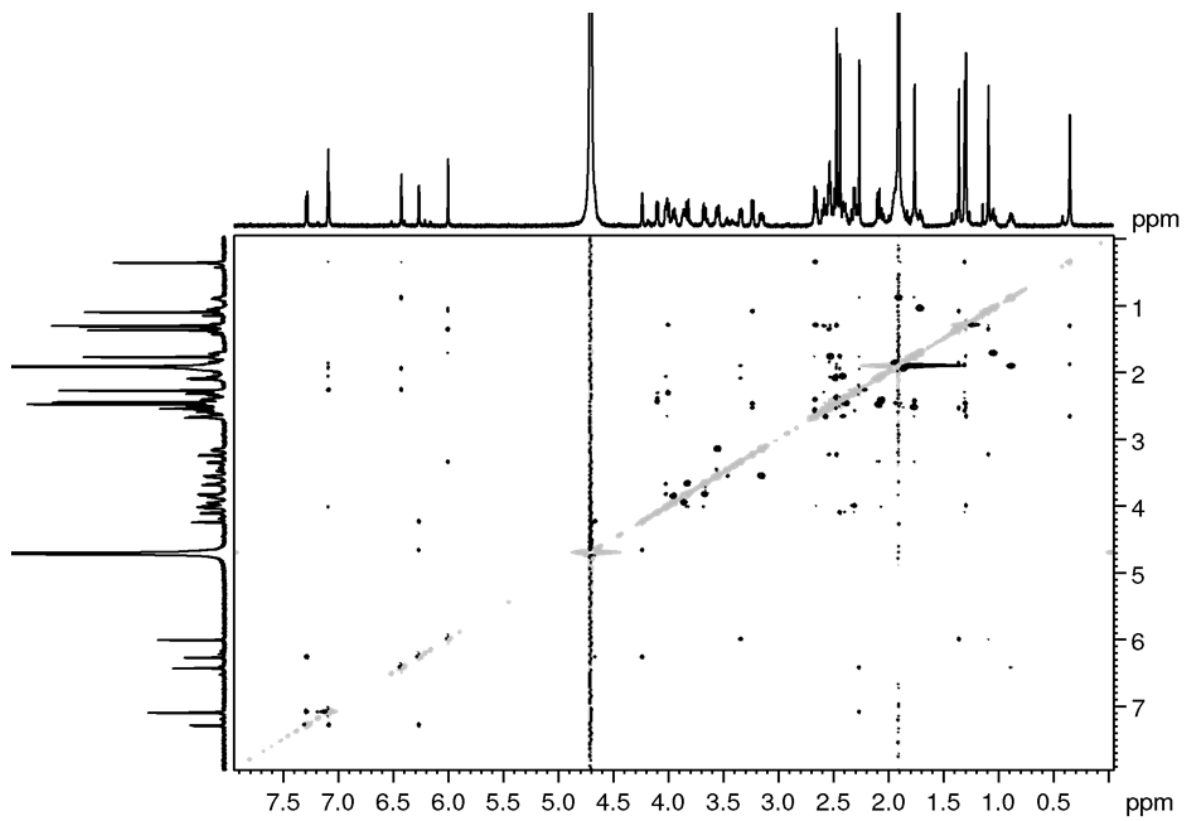


**Fig. S21:**  $^1\text{H}$ - $^1\text{H}$  ROESY spectrum of the 5-MeBza-NCba.

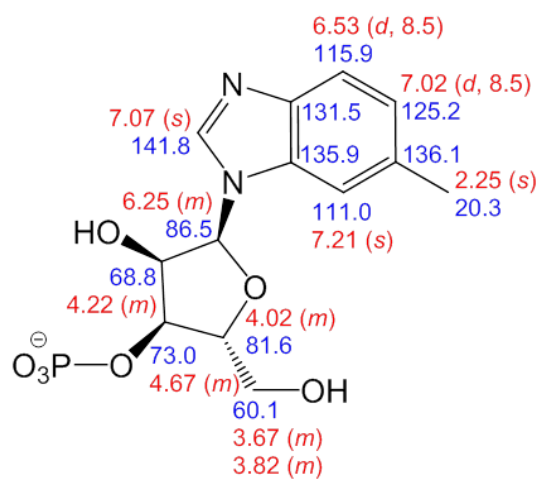


**Fig. S22:** Chemical shifts ( $\delta_H$  red,  $\delta_C$  blue) of the 6-MeBza-*N*- $\alpha$ -ribofuranosyl-fragment.

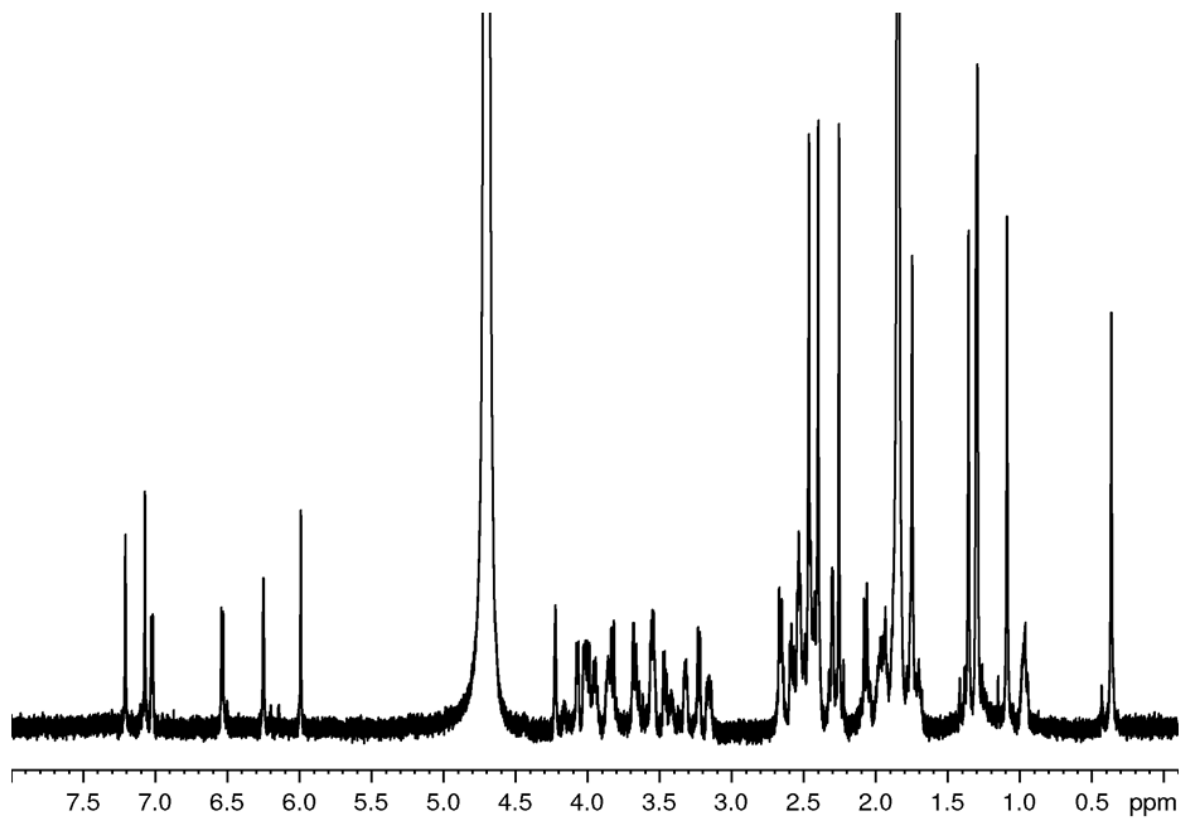


**Fig. S23:** <sup>1</sup>H-NMR spectrum of the 6-MeBza-NCba.

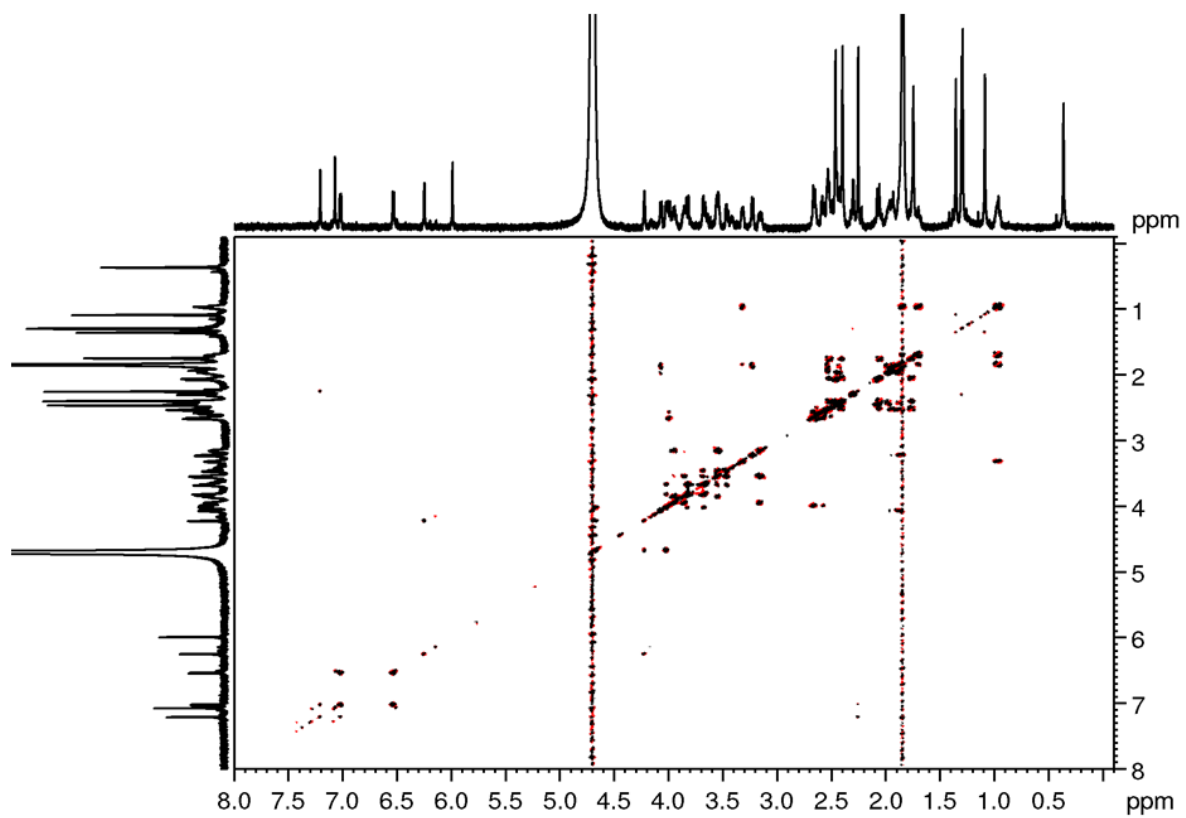


**Fig. S24:**  $^1\text{H}$ - $^1\text{H}$ -DQFCOSY spectrum of the 6-MeBza-NCba.

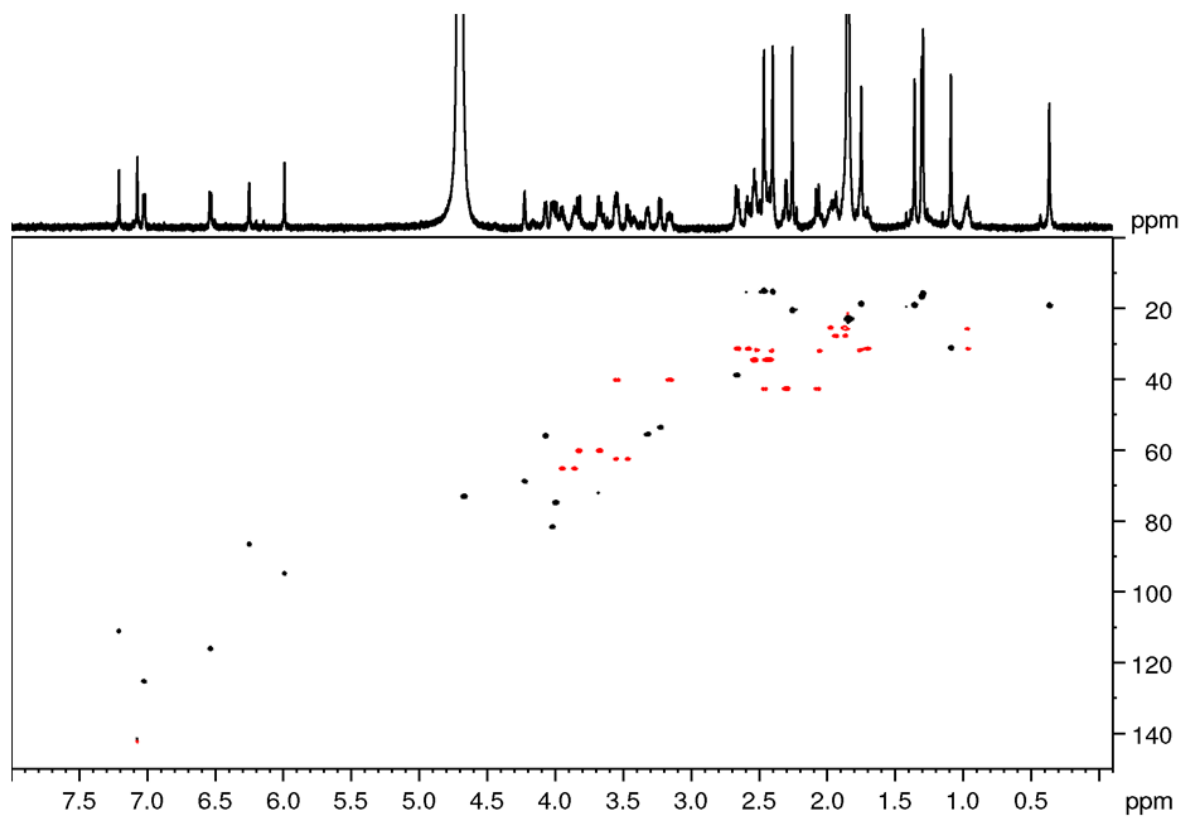


**Fig. S25:**  $^1\text{H}$ - $^{13}\text{C}$  HSQC spectrum of 6-MeBza-NCba.

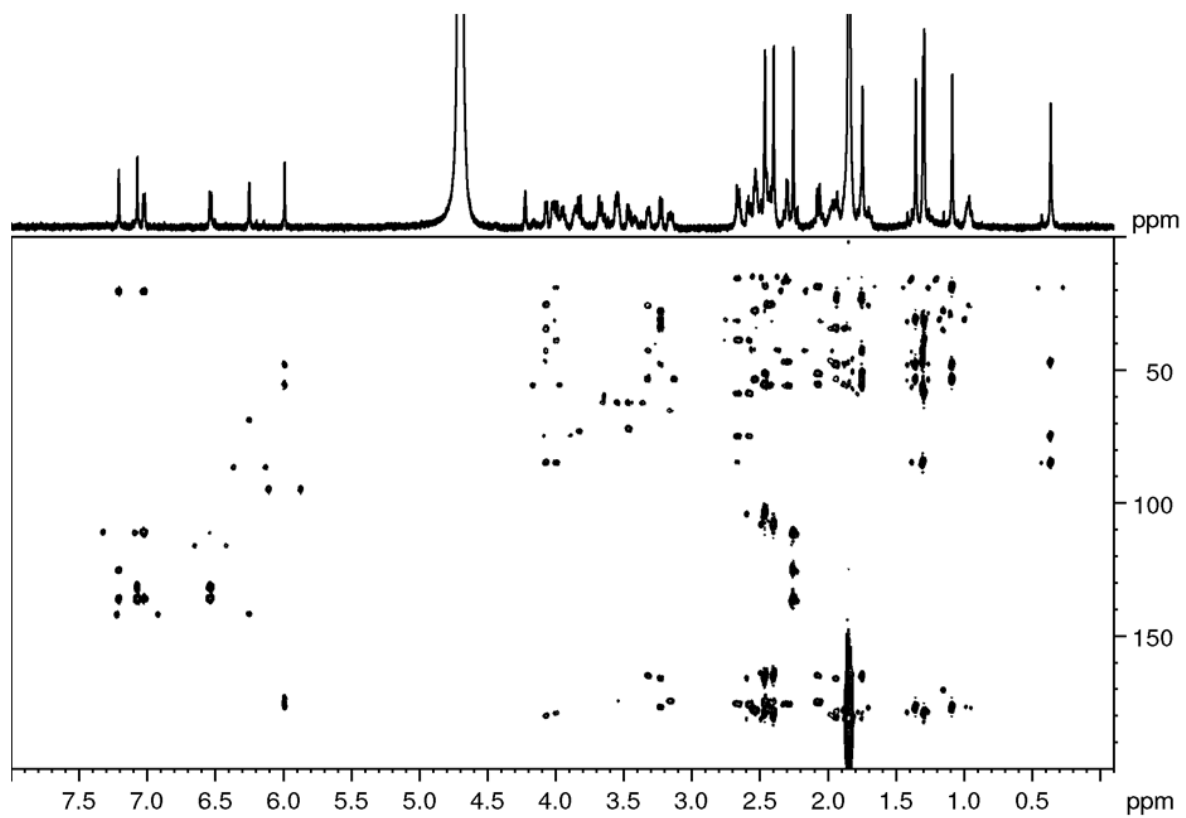


**Fig. S26:**  $^1\text{H}$ - $^{13}\text{C}$  HMBC spectrum of the 6-MeBza-NCba.

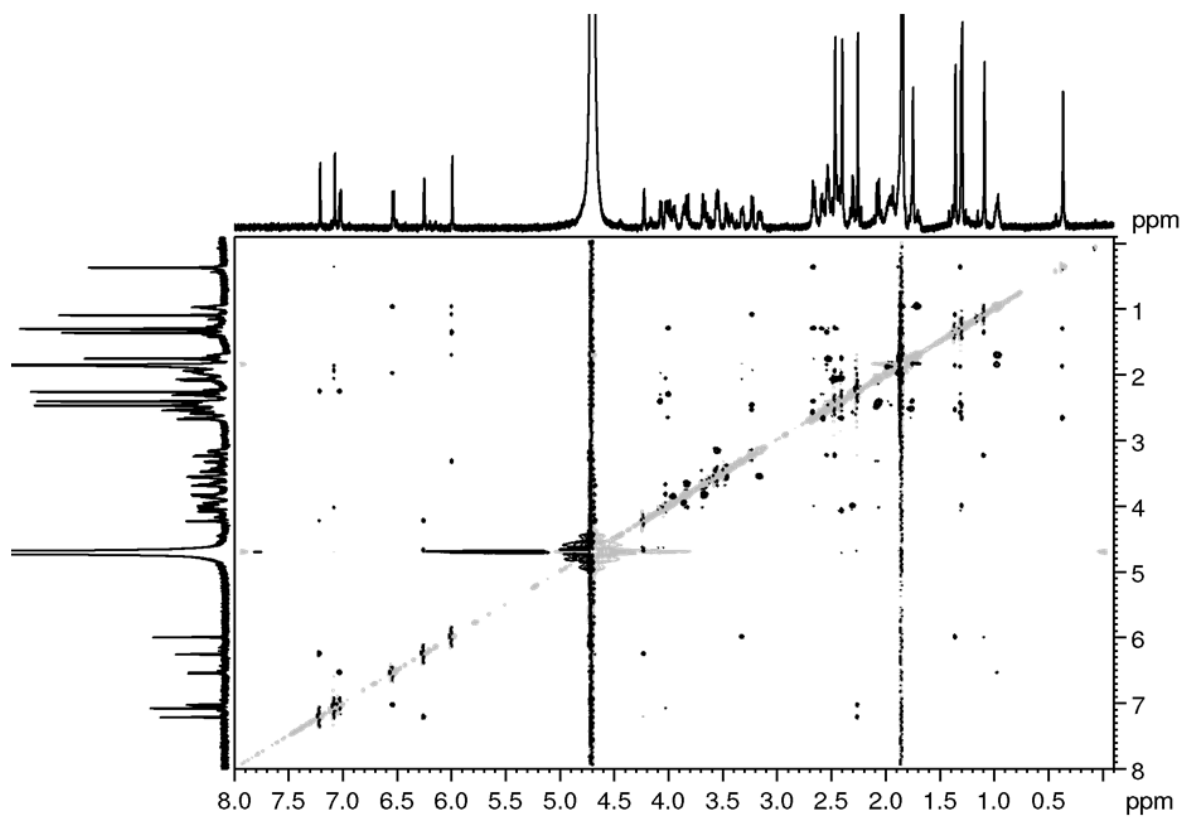


**Fig. S27:**  $^1\text{H}$ - $^1\text{H}$  ROESY spectrum of the 6-MeBza-NCba.

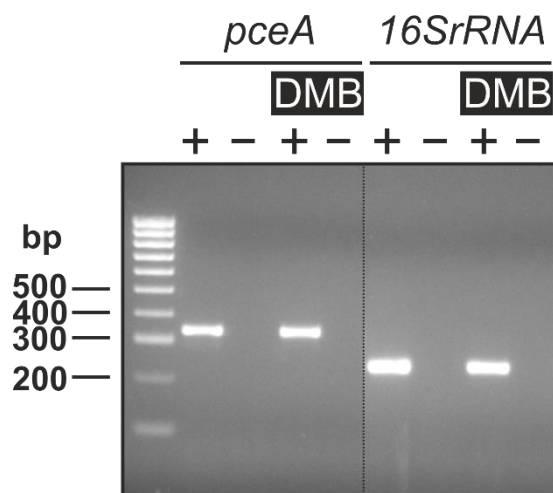


**Fig. S28:** Transcript level of the *pceA* gene in PCE-grown *S. multivorans* cultivated in the presence of DMB detected by reverse transcriptase PCR. The housekeeping gene *16SrRNA* was used as a control. (+) = with reverse transcription / (-) = without reverse transcription. Total RNA of *S. multivorans* ( $10^9$  cells) was extracted with the RNeasy Mini Kit (Qiagen, Hilden, Germany) and applied to DNA digestion with DNase I (Roche, Mannheim, Germany) at 37°C for 1 h. RNA concentration was determined with a Qubit® 1.0 Fluorometers (Invitrogen, Darmstadt, Germany) and the Qubit® RNA BR Assay Kit (Thermo Fisher Scientific, Braunschweig, Germany). The reverse transcriptase (RT) reaction was performed with 1 µg total RNA using the OneStep RT-PCR Kit (Qiagen, Hilden, Germany) at 50°C for 1 h. The subsequent PCR was run as follows: initial activation (15 min, 95°C) and 20 cycles of polymerization (1 min 94°C; 30 sec 50°C; 1 min 72°C). The following primers were used: 5'-ACACATTAAAAAATAAATAACTGTACTTGGGG-3' and 5'-TGAGTAAACGCTGTTCGTA CTTCCAGC-3' for *pceA* (fragment size: 339 bp) and 5'-GAGACACGGTCCAGACTCCTAC-3' and 5'-CTCGACTTGATTTCCAGCCTAC-3' for *16SrRNA* (fragment size: 255 bp).



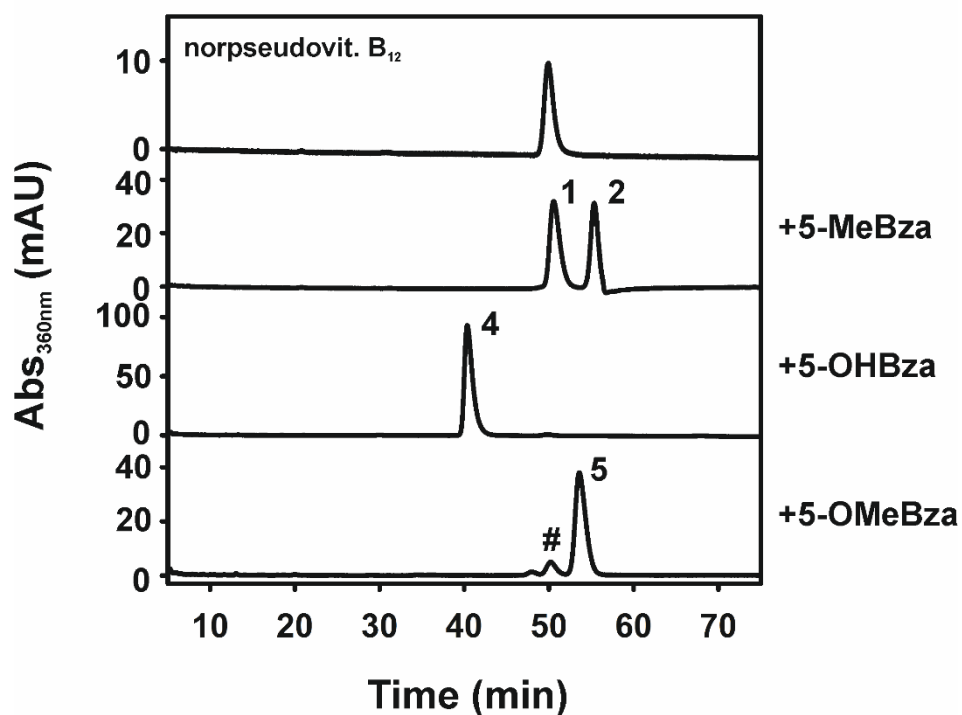


**Fig. S29:** HPLC-elution profiles of NCbas extracted from PceA purified from *S. multivorans* GD21 cultivated in the presence of either 5-MeBza, 5-OHBza, or 5-OMeBza. The first chromatogram shows a norpseudovitamin B<sub>12</sub> standard. The designations of the signals refer to the NCbas identified in the respective cell types (see Fig. 1C). The specific activities of the purified PceA enzymes were as follows: + 5-MeBza, 687 nkat/mg; + 5-OHBza, 1056 nkat/mg; + 5-OMeBza, 1504 nkat/mg.

**Tab. S2:** Data collection and refinement statistics.

	PceA harboring <b>6-OHBza</b> -norcobamide	PceA harboring <b>5-OMeBza</b> -norcobamide
<b>Data Collection</b>	PETRA III P11	HZB-MX 14.1
Wavelength (Å)	0.9184	0.9184
Resolution range (Å)	36.1 - 1.59 (1.65 - 1.59)	39.8 - 1.60 (1.66 - 1.60)
Space group	<i>P</i> 4 <sub>1</sub>	<i>P</i> 4 <sub>1</sub>
Unit cell (Å, °)	73.6 73.6 184.7 90 90 90	73.6 73.6 185.3 90 90 90
Unique reflections	129361 (12146)	129127 (12767)
Multiplicity	13.2 (12.6)	13.8 (13.6)
Completeness (%)	99 (93)	100 (99)
I/sigma(I)	14.9 (1.9)	19.0 (1.7)
Wilson B-factor (Å <sup>2</sup> )	19.0	20.2
R-merge	0.114 (0.931)	0.098 (1.57)
R-pim	0.033 (0.270)	0.027 (0.436)
CC <sub>1/2</sub>	1.00 (0.80)	1.00 (0.62)
<b>Refinement</b>		
R-work	0.152 (0.257)	0.151 (0.260)
R-free	0.177 (0.285)	0.172 (0.289)
Number of non-H atoms	7945	7820
macromolecules	6838	6843
ligands	243	251
solvent	864	726
Protein residues	862	865
RMS(bonds, Å)	0.007	0.007
RMS(angles, °)	0.93	0.93
Ramachandran favored (%)	98	98
Ramachandran outliers (%)	0	0
Rotamer outliers (%)	0	0
Clashscore	2.7	2.4
Average B-factor (Å <sup>2</sup> )	26.5	26.2
macromolecules	25.5	25.4
ligands	21.7	21.7
solvent	36.0	35.1